



# Effect of adding Ge on rapid whisker growth of Sn–3Ag–0.5Cu–0.5Ce alloy

Tung-Han Chuang\*, Chih-Chien Chi<sup>1</sup>

Institute of Materials Science and Engineering, National Taiwan University, No. 1, Section 4, Roosevelt Road, Taipei, 10617, Taiwan, ROC

## ARTICLE INFO

### Article history:

Received 29 September 2008  
Received in revised form 23 February 2009  
Accepted 24 February 2009  
Available online 9 March 2009

### Keywords:

Tin whiskers  
Rare earth element  
Oxidation resistance  
Sn–3Ag–0.5Cu–0.5Ce–0.5Ge

## ABSTRACT

Although solders doped with rare earth elements have been reported to show many beneficial effects, tin whisker growth has been observed to grow at an extremely high rate on the surface of such novel solder alloys. This study shows that adding 0.5 wt.% Ge into a Sn–3Ag–0.5Cu–0.5Ce alloy effectively decreased whisker growth. This inhibition effect is attributed to alleviation of oxidation in the CeSn<sub>3</sub> intermetallic phase in this alloy as a result of Ge-alloying. Compressive stress in this case is insufficient to extrude tin atoms out of the solder to form whiskers.

© 2009 Elsevier B.V. All rights reserved.

## 1. Introduction

Benefits of adding rare earth elements into solder alloys, such as enhanced wettability and mechanical properties, have been reported [1–4]. However, Chuang and Yen observed tin whiskers in a Sn–3Ag–0.5Cu–0.5Ce solder alloy after air-exposure at room temperature; maximum whisker growth rate was 0.9 nm/s [5], which is significantly higher than previously reported typical growth rates (0.001–0.01 nm/s) of tin whiskers in bulk materials [6]. In the literature, certain cases of rapid whisker growth can also be found: Tu and Li calculated the growth rate of beta-Sn whiskers to be at roughly 0.26 mm/year (around 0.008 nm/s) based on a grain boundary fluid-flow mechanism [7]. Chen and Wilcox identified tin whisker growth rates of about 0.2–0.4 nm/s on electroplated Sn–Mn films [8]. Liu et al. determined that whisker growth on Sn film can be accelerated by applying electrical currents; the whisker growth rate was 0.3 nm/s at a current density of  $1.5 \times 10^5$  A/cm<sup>2</sup> [9]. It seems that the observations of Chuang and Yen [5] in their study on rare-earth-doped Sn–3Ag–0.5Cu–0.5Ce solder alloy have shed light on the shortest nucleation times and highest growth rates in the research field of tin whiskers. Further investigations showed that the morphology of fiber-shaped whiskers (0.1–0.3 μm in diameter) changed to coarse hillock-shaped whiskers (1–3 μm in diameter) when storage temperature increased from 25 °C to 150 °C [10], and both fiber- and hillock-shaped whiskers appeared in Sn–3Ag–0.5Cu solders doped

with 0.1–1.0 wt.% Ce [11]. According to the mechanism proposed by Chuang [12], such whisker growth is attributed to oxidation of peritectic CeSn<sub>3</sub> intermetallics, which release tin atoms. Compressive stress resulting from volume expansion of oxidized CeSn<sub>3</sub> clusters extrudes tin atoms out of the surface of Ce-doped Sn–3Ag–0.5Cu solder alloy. Dudek and Chawla observed a similar phenomenon in that selective oxidation of CeSn<sub>3</sub> generates compressive stress that forms tin whiskers on Sn–3.9Ag–0.7Cu–2Ce solder alloy [13]. It is known that the appearance of tin whiskers in solder joints can cause short circuits in electronic products. Consequently, many efforts have been made since the discovery of the amazingly rapid growth of tin whiskers to find a way to restrict the growth without degrading the beneficial effects of rare earth elements on Pb-free solders.

Recently, Chuang and Lin made progress in the above area by adding 0.5 wt.% Zn into a Sn–3Ag–0.5Cu–0.5Ce alloy [14]. According to their results, the CeSn<sub>3</sub> intermetallic phase in such a Sn–3Ag–0.5Cu–0.5Ce–0.5Zn solder alloy was more than 10-fold finer than that in Sn–3Ag–0.5Cu–0.5Ce. Due to their small size, CeSn<sub>3</sub> intermetallic compounds cannot provide sufficient tin atoms or compressive stress to induce the formation of either fiber-shaped or hillock-shaped whiskers. Since whisker growth on the surface of rare-earth-doped solder alloys is correlated with oxidation of CeSn<sub>3</sub> intermetallic compounds, and since germanium is a well-known alloying element that improves solder oxidation resistance [15–19], the inhibition effect of adding Ge on the whisker growth of Sn–3Ag–0.5Cu–0.5Ce is considered.

## 2. Experimental

For the experiments, Sn–3Ag–0.5Cu–0.5Ce and Sn–3Ag–0.5Cu–0.5Ce–0.5Ge alloys were prepared via induction melting a Sn–6.6 wt.% Ce master alloy at 1000 °C

\* Corresponding author. Tel.: +886 2 23929635; fax: +886 2 23929635.  
E-mail addresses: [tunghan@ntu.edu.tw](mailto:tunghan@ntu.edu.tw) (T.-H. Chuang), [f93527062@ntu.edu.tw](mailto:f93527062@ntu.edu.tw) (C.-C. Chi).

<sup>1</sup> Tel.: +886 2 23671979; fax: +886 2 23929635.

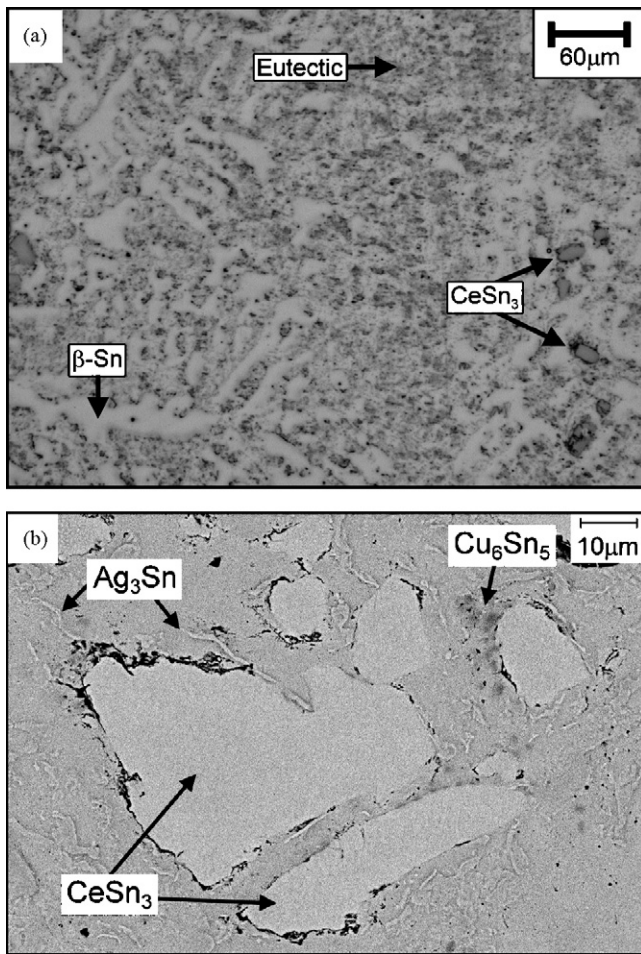


**Fig. 1.** Microstructure of the as-cast Sn–3Ag–0.5Cu–0.5Ce solders: (a) low magnification, (b) high magnification.

in a quartz tube under vacuum ( $10^{-5}$  Torr). During the melting process, the quartz tube was flipped multiple times to ensure alloying element uniformity. The quartz tube with the molten alloy was then quenched in cold water. The Sn–6.6 wt.% Ce master alloy was encapsulated in a new quartz tube together with elements Sn, Ag, Cu and Ge under  $10^{-5}$  vacuum and then remelted and quenched using the same process. The solidified ingots were cross-sectioned into specimens sized roughly  $10\text{ mm} \times 10\text{ mm} \times 20\text{ mm}$ , polished, and then stored at room temperature in air. Some specimens were heated to  $150^\circ\text{C}$  in an air furnace. The microstructure of the solder alloys and the morphology of the tin whiskers that formed on air-stored specimens were observed via scanning electron microscopy (SEM). The chemical compositions of metallographic phases and oxidation layers were analyzed using an electron probe microanalyzer (EPMA).

### 3. Results and discussion

The microstructures of as-cast Sn–3Ag–0.5Cu–0.5Ce and Sn–3Ag–0.5Cu–0.5Ce–0.5Ge solder alloys, as shown in Figs. 1 and 2, contain  $\text{Ag}_3\text{Sn}$ ,  $\text{Cu}_6\text{Sn}_5$  and  $\text{CeSn}_3$  phases. The  $\text{CeSn}_3$  intermetallic compounds appeared as large clusters in the solder matrix and may result from the very low solubility of Ce in Sn. In our labo-

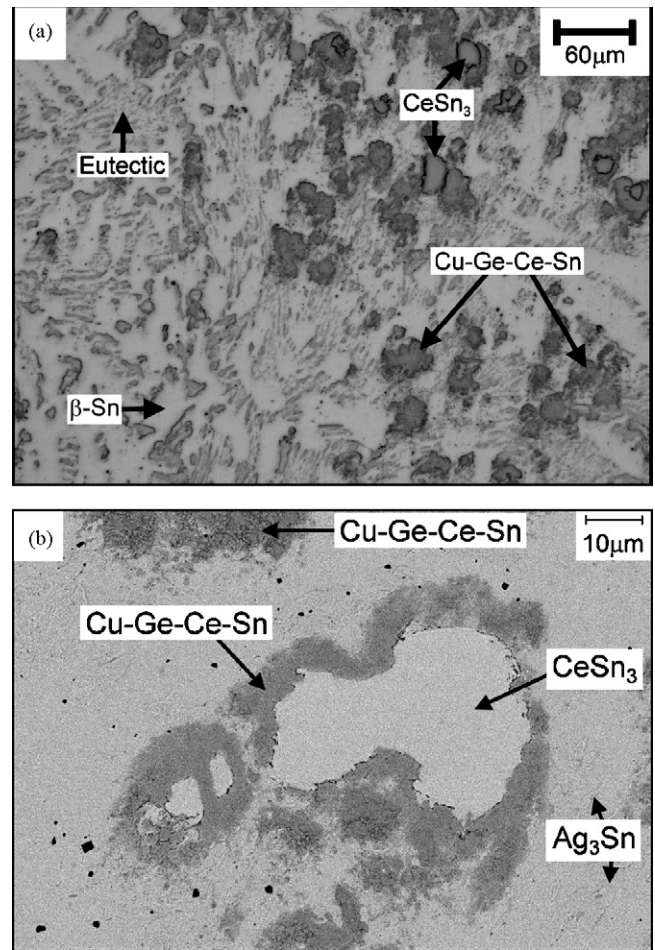


**Fig. 2.** Microstructure of the as-cast Sn–3Ag–0.5Cu–0.5Ce–0.5Ge solders: (a) low magnification, (b) high magnification.

ratory, these solder alloys were used as solder balls in ball grid array (BGA) packages, which were reflowed at  $250^\circ\text{C}$  and solidified via air cooling. The microstructure of these  $\text{CeSn}_3$  clusters in BGA solder balls after reflowing resembled those in the ingots. It is evidenced that the formation of large cluster-shaped  $\text{CeSn}_3$  intermetallic compounds was independent of the cooling rate during the solidification process of the molten solders.

The chemical compositions of these  $\text{CeSn}_3$  intermetallic clusters were analyzed and listed in Table 1. Roughly 0.41 at.% Ge replaced the Sn atoms in the  $\text{CeSn}_3$  phase of the Sn–3Ag–0.5Cu–0.5Ce–0.5Ge solder. Additional phases appeared in the solder matrix and around the  $\text{CeSn}_3$  intermetallic clusters in this alloy containing Ge (Fig. 2). The EPMA analyses indicate that the phases that formed at both locations had similar compositions, largely Cu and Ge with minor amounts of Ce and Sn, as shown in Table 1. Based on the related phase diagrams [20], we suggest that as the Sn–3Ag–0.5Cu–0.5Ce–0.5Ge solder alloy cooled from  $1000^\circ\text{C}$ , the  $\text{CeSn}_3$  intermetallic clusters solidified from the molten alloy

**Table 1**  
Chemical compositions of various phases formed in Sn–3Ag–0.5Cu–0.5Ce and Sn–3Ag–0.5Cu–0.5Ce–0.5Ge solder.

Specimens	Phase	Compositions (at.%)				
		Sn	Ag	Cu	Ce	Ge
Sn–3Ag–0.5Cu–0.5Ce	$\text{CeSn}_3$	74.11	0.51	–	25.38	–
Sn–3Ag–0.5Cu–0.5Ce–0.5Ge	$\text{CeSn}_3$	73.66	0.48	0.09	25.36	0.41
Sn–3Ag–0.5Cu–0.5Ce–0.5Ge	Cu–Ge–Ce–Sn in solder matrix	10.46	0.36	37.53	18.31	33.34
Sn–3Ag–0.5Cu–0.5Ce–0.5Ge	Cu–Ge–Ce–Sn around $\text{CeSn}_3$	13.23	0.38	36.31	17.73	32.35

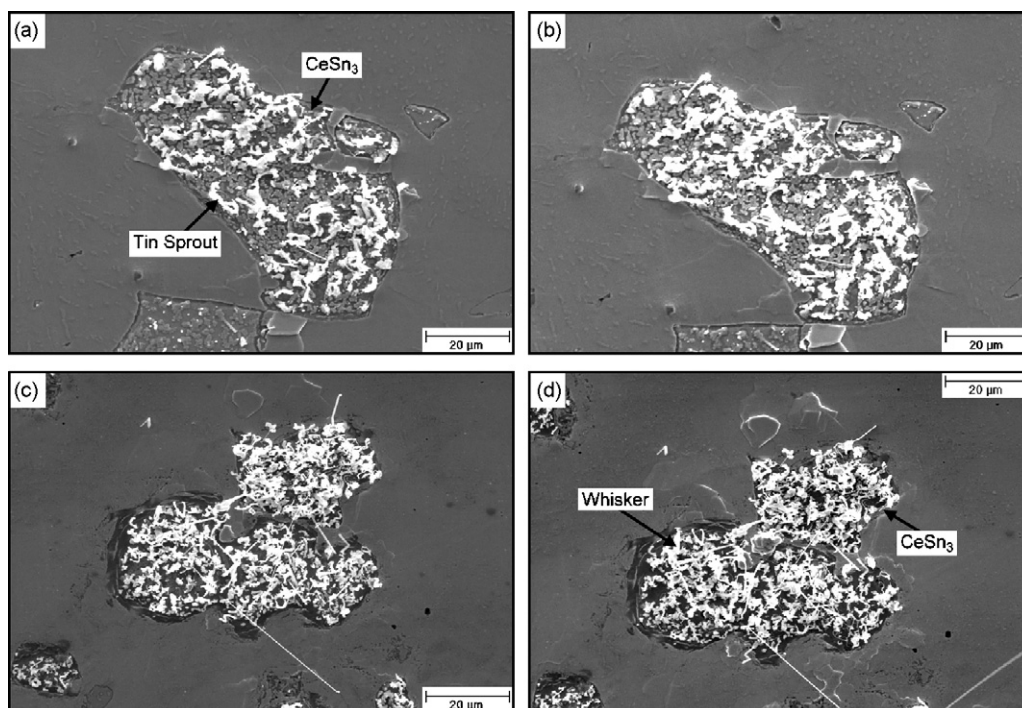


Fig. 3. Tin whisker growth in Sn-3Ag-0.5Cu-0.5Ce solders after air exposure at room temperature for (a) 12 h, (b) 58 h, (c) 170 h and (d) 674 h.

at the start of the Ce-Sn peritectic reaction. The other intermetallic compounds, such as  $\text{CeSn}_3$ ,  $\text{Ce}_x\text{Ge}_y$ ,  $\text{Ce}_x\text{Cu}_y$  and  $\text{GeCu}_3$  ( $\epsilon$  phase), subsequently formed and tended to segregate on the surfaces of  $\text{CeSn}_3$  clusters. Some Ce and Sn atoms of the  $\text{CeSn}_3$  intermetallic phase diffused into the Cu-Ge-Ce outer shell, forming Cu-Ge-Ce-Sn envelopes. In certain cases,  $\text{CeSn}_3$  intermetallic compounds reacted completely with the Cu-Ge-Ce phase, resulting in isolated Cu-Ge-Ce-Sn clusters. The microstructures of

both solder alloys, as compared in Figs. 1b and 2b, indicate that the  $\text{CeSn}_3$  intermetallic clusters in the Sn-3Ag-0.5Cu-0.5Ce alloy were roughly  $50\ \mu\text{m}$  in size, which is larger than those in Sn-3Ag-0.5Cu-0.5Ce-0.5Ge. However, the  $\text{CeSn}_3$  clusters combined with the Cu-Ge-Ce-Sn envelopes were similar in size to those of the  $\text{CeSn}_3$  intermetallic compounds in the Sn-3Ag-0.5Cu-0.5Ce solder alloy, confirming the suggestion regarding the formation of Cu-Ge-Ce-Sn phases.

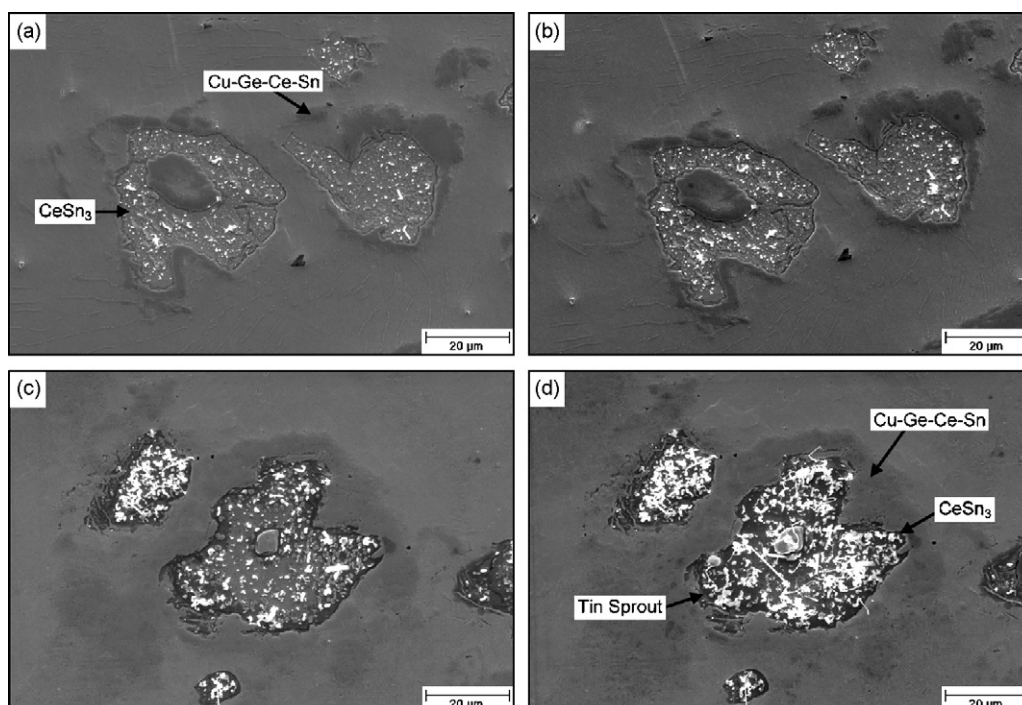


Fig. 4. Tin whisker growth in Sn-3Ag-0.5Cu-0.5Ce-0.5Ge solders after air exposure at room temperature for (a) 12 h, (b) 58 h, (c) 170 h and (d) 674 h.

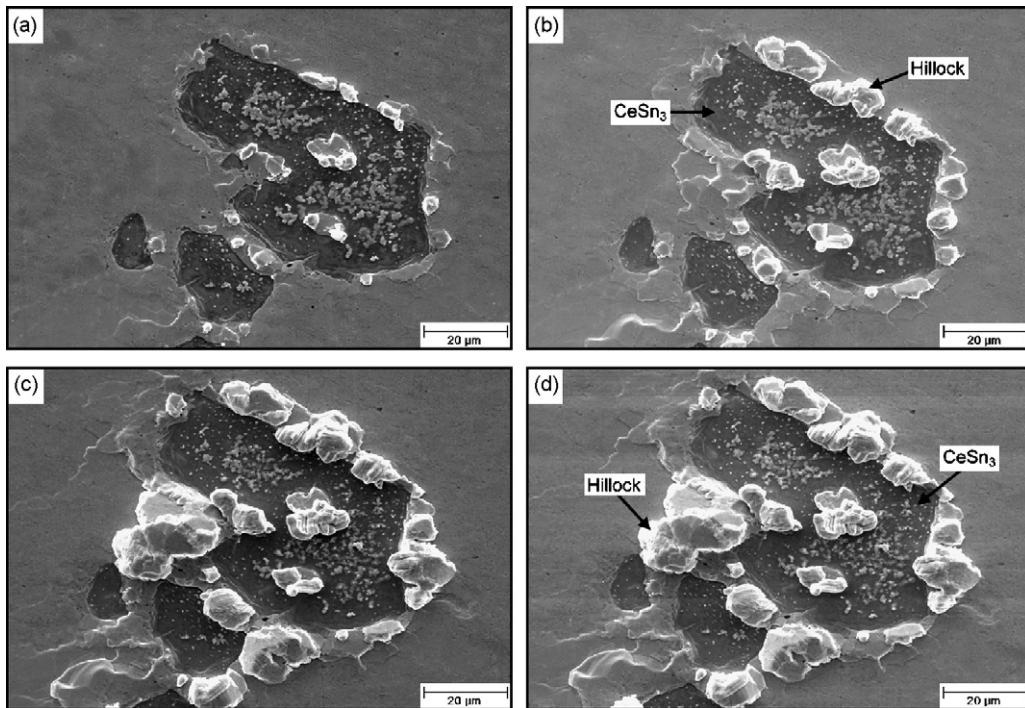


Fig. 5. Tin whisker growth in Sn-3Ag-0.5Cu-0.5Ce solders after air exposure at 150 °C for (a) 15 min, (b) 3 h, (c) 146 h and (d) 315 h.

Fig. 3a shows that in the Sn-3Ag-0.5Cu-0.5Ce solder, many tin sprouts appeared on the surface of  $\text{CeSn}_3$  intermetallics after air-exposure at room temperature for only 12 h. Conversely, only a small number of very tiny tin sprouts existed in the Sn-3Ag-0.5Cu-0.5Ce-0.5Ge alloy (Fig. 4a). Increasing air-storage time caused rapid formation of long fiber-shaped whiskers in Sn-3Ag-0.5Cu-0.5Ce solder (Fig. 3). The morphology of these fiber-shaped whiskers has been described by Chuang and Yen [5].

In contrast, the tin sprouts in Sn-3Ag-0.5Cu-0.5Ce-0.5Ge grew less than short whiskers, even after long-term exposure at room temperature for 674 h (Fig. 4d). Obviously, whisker growth in Sn-3Ag-0.5Cu-0.5Ce solder alloy stored at room temperature was inhibited by adding 0.5 wt.% Ge.

Furthermore, raising the air-storage temperature to 150 °C for 3 h generated many coarse hillock-shaped whiskers around the  $\text{CeSn}_3$  intermetallic clusters in the Sn-3Ag-0.5Cu-0.5Ce solder

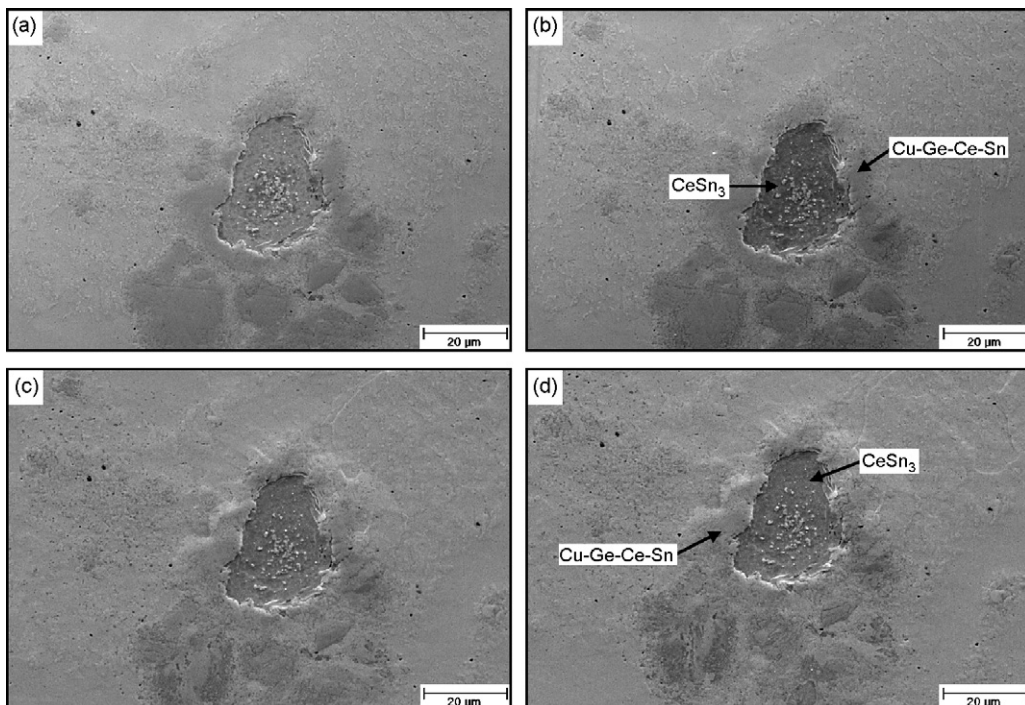


Fig. 6. Tin whisker growth in Sn-3Ag-0.5Cu-0.5Ce-0.5Ge solders after air exposure at 150 °C for (a) 15 min, (b) 3 h, (c) 146 h and (d) 315 h.

alloy, as shown in Fig. 5a. These tin hillocks grew to a large size after air exposure at 150 °C for 3 h and 146 h, respectively. Conversely, Fig. 6 shows that no hillocks existed on the surface of Sn–3Ag–0.5Cu–0.5Ce–0.5Ge solder alloy. The microstructure of Sn–3Ag–0.5Cu–0.5Ce–0.5Ge alloy remained almost unchanged even after long-term exposure at 150 °C for 315 h (Fig. 6d). In this case, many giant hillocks were extruded out of the Ge-free Sn–3Ag–0.5Cu–0.5Ce alloy, and the solder matrix near the CeSn<sub>3</sub> clusters was pushed into a convex morphology (Fig. 5d). Experimental results indicate that whisker growth can be inhibited completely in Sn–3Ag–0.5Cu–0.5Ce–0.5Ge solder when stored in air at 150 °C.

Another study of Sn–3Ag–0.5Cu–0.5Ce–0.5Zn solder alloy [14] demonstrated that refining the CeSn<sub>3</sub> intermetallic phase inhibits whisker growth due to insufficient tin atoms and compressive stress after oxidation reactions. The CeSn<sub>3</sub> intermetallic compounds in Sn–3Ag–0.5Cu–0.5Ce–0.5Ge solder were slightly smaller in size than those in Ge-free alloy (Figs. 1 and 2). However, the sizes of CeSn<sub>3</sub> clusters in Sn–3Ag–0.5Cu–0.5Ce–0.5Ge solder were still large enough to create sufficient tin atoms and compressive stress for the whisker growth. The size effect for the example Sn–3Ag–0.5Cu–0.5Ce–0.5Zn solder alloy [14] may not be the primary cause of inhibited tin-whisker growth in the Sn–3Ag–0.5Cu–0.5Ce–0.5Ge solder. Another proposed interpretation is the effect of alleviating oxidation in Ge alloying in solders, which has been widely reported and applied in the development of Pb-free solders [15–19].

In the electronics industry, it is well known that discoloring on the surface of solder joints, which is caused by oxidation of molten solders, can be reduced by adding Ge. Cho et al. observed

that the surface of Sn–3Ag–0.5Cu–0.05Ge solder alloy retained its luster after reflowing multiple times [15]. Chemical analyses via X-ray photoelectron spectrometry (XPS) demonstrate that Ge existed on the surface of the Sn–3Ag–0.5Cu–0.25Ge solder. Cho et al. suggested that such a thin GeO<sub>x</sub> film prevented solder oxidation and discoloring. Lee et al. added 0.007 wt.% Ge to Sn–3Ag–0.5Cu solder alloy, aged specimens at 175 °C for 9 h, and analyzed the samples using Auger electron spectrometry (AES). They determined that the concentration profile of oxygen in this Ge-doped alloy declined dramatically as specimen surface depth increased [16]. Lalena et al. added 0.05 wt.% Ge into Bi–11Ag solder alloy and identified that a GeO<sub>2</sub> film appeared on the surface in preference to Bi<sub>2</sub>O<sub>3</sub> oxides due to the lower formation of free energy of GeO<sub>2</sub> (–98 kcal/mol) compared with that of Bi<sub>2</sub>O<sub>3</sub> (–69 kcal/mol), and that such a GeO<sub>2</sub> film can effectively inhibit the oxidation of solder alloy [17]. Gong and Xian studied the oxidation resistance of molten Sn alloyed with various amounts of Ge at 250 °C. They found that the cross of solder alloy decreased as the amount of Ge added increased [18]. The XPS analyses showed that very high Ge content appeared on the surface of oxidized solder alloy in this study. In contrast, the Sn concentration decreased as the amount of Ge on the solder surface increased. Gong and Xian suggested that formation of a protective Ge-oxide film on the surface prevented oxygen reacting with liquid Sn, which decreased cross during melting. They also found that Sn had lower oxidation resistance when the amount of Ge added was

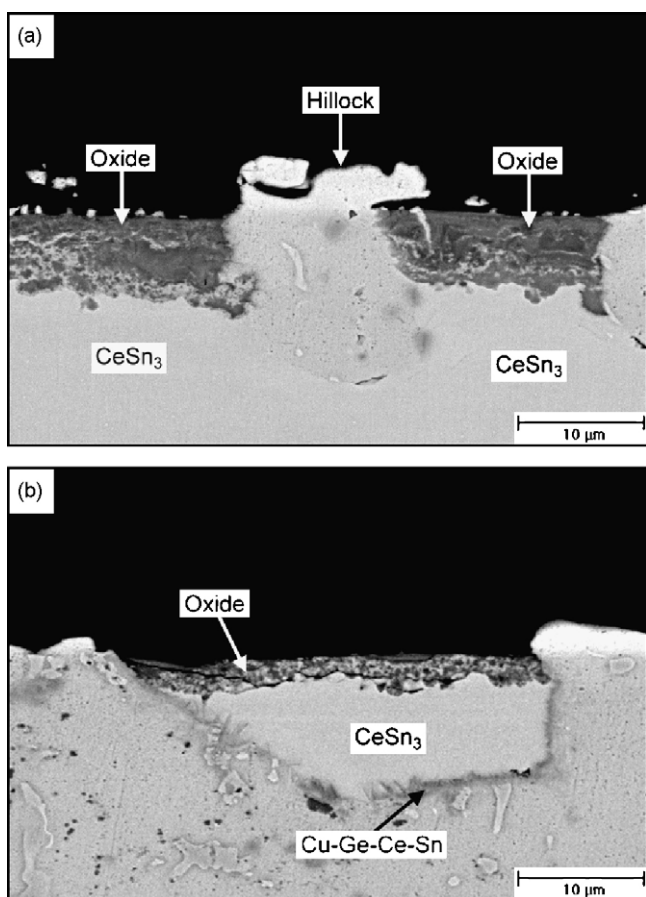


Fig. 7. Cross-section of the oxidized CeSn<sub>3</sub> phases in (a) Sn–3Ag–0.5Cu–0.5Ce and (b) Sn–3Ag–0.5Cu–0.5Ce–0.5Ge solders after storage at 150 °C for 46 h in air furnace.

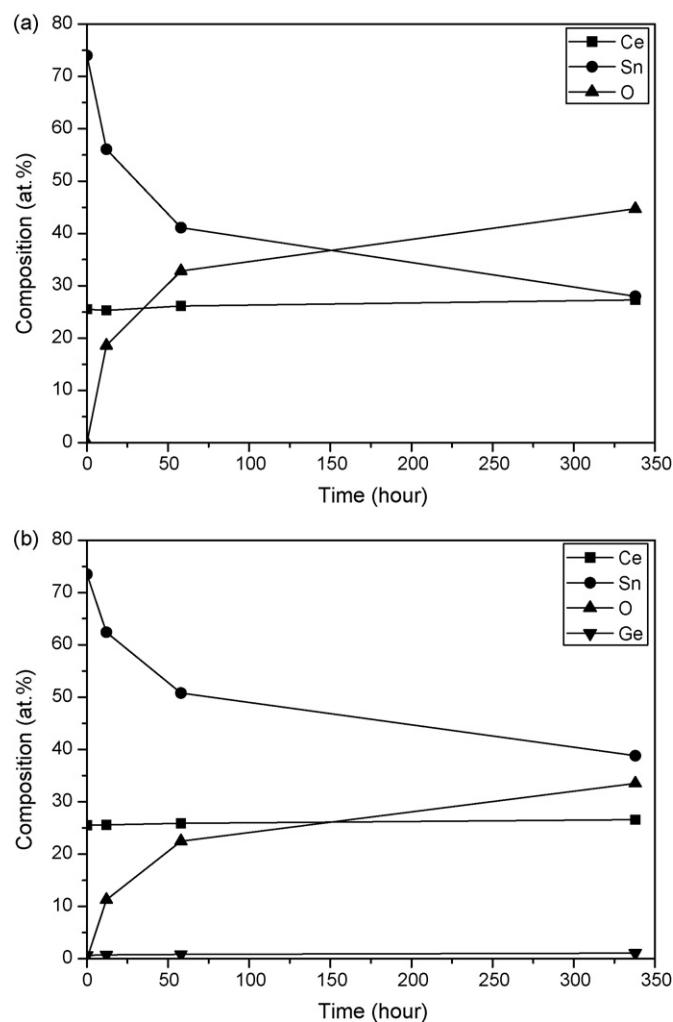
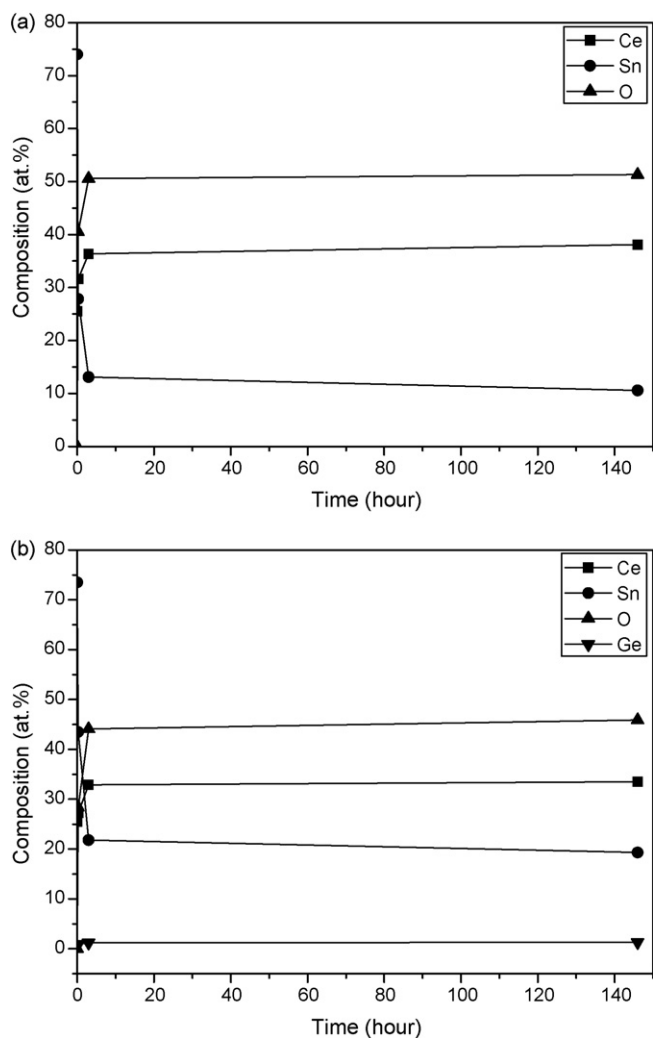
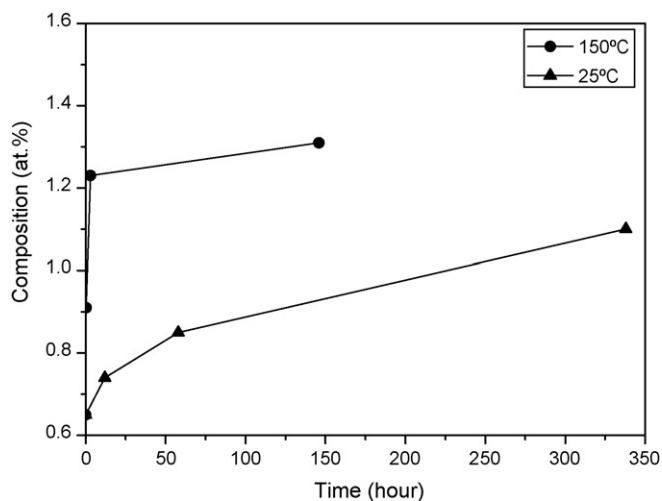


Fig. 8. Composition profiles of the surface of CeSn<sub>3</sub> phase in (a) Sn–3Ag–0.5Cu–0.5Ce and (b) Sn–3Ag–0.5Cu–0.5Ce–0.5Ge solders stored at room temperature in air for various time periods.



**Fig. 9.** Composition profiles of the surface of  $\text{CeSn}_3$  phase in (a)  $\text{Sn-3Ag-0.5Cu-0.5Ce}$  and (b)  $\text{Sn-3Ag-0.5Cu-0.5Ce-0.5Ge}$  solders stored at 150 °C in air for various time periods.

lower than the saturated solubility of Ge (0.0042 at.%) in molten Sn at 250 °C. However, when the amount of Ge exceeded the solubility level, excess Ge migrated to the liquid solder surface, forming a Ge-oxide film. When the Ge-oxide film completely covers the molten



**Fig. 10.** Ge content on the surface of oxidized  $\text{CeSn}_3$  intermetallic clusters during air-storage at room temperature and at 150 °C for various time periods.

solder, its oxidation resistance increases markedly. A similar effect has been reported by Habu et al., who demonstrated that the rate of dross formation on molten  $\text{Sn-2Ag-4Bi-0.5Cu-0.1Ge}$  solder was slower than that on Ge-free alloy [19].

To confirm the improvement in oxidation resistance of the  $\text{Sn-3Ag-0.5Cu-0.5Ce-0.5Ge}$  solder in comparison with that of  $\text{Sn-3Ag-0.5Cu-0.5Ce}$ , specimens of both alloys were cross-sectioned across the oxidized  $\text{CeSn}_3$  intermetallic compounds after storage at 150 °C for 46 h in an air furnace. It can be clearly observed in Fig. 7 that the oxide layer on the outer surface of the  $\text{Sn-3Ag-0.5Cu-0.5Ce-0.5Ge}$  solder is much thinner than that on the Ge-free  $\text{Sn-3Ag-0.5Cu-0.5Ce}$  alloy under the same air-exposure conditions. Additionally, the EPMA analyses, shown in Fig. 8, reveal that the oxygen content on the surface of  $\text{CeSn}_3$  intermetallic clusters in the  $\text{Sn-3Ag-0.5Cu-0.5Ce}$  and  $\text{Sn-3Ag-0.5Cu-0.5Ce-0.5Ge}$  solder alloys increased rapidly to 33 at.% and 22 at.%, respectively, after air storage at room temperature for 58 h. The oxygen content increased gradually to roughly 40 at.% and 34 at.% for  $\text{Sn-3Ag-0.5Cu-0.5Ce}$  and  $\text{Sn-3Ag-0.5Cu-0.5Ce-0.5Ge}$  solder alloys, respectively, after long-term exposure for 338 h. Fig. 9 shows that increasing the air storage temperature to 150 °C for 3 h caused the amount of oxygen on the surface of  $\text{CeSn}_3$  intermetallic compounds in  $\text{Sn-3Ag-0.5Cu-0.5Ce}$  and  $\text{Sn-3Ag-0.5Cu-0.5Ce-0.5Ge}$  solder alloys to increase rapidly to about 51 at.% and 45 at.%, respectively, which remained almost constant as storage time was increased. It is obvious that the surfaces of  $\text{CeSn}_3$  intermetallic clusters in  $\text{Sn-3Ag-0.5Cu-0.5Ce-0.5Ge}$  alloy were oxidized less than those in the Ge-free  $\text{Sn-3Ag-0.5Cu-0.5Ce}$  solder. On the other hand, the amount of Ge on the surface of oxidized  $\text{CeSn}_3$  intermetallics in the  $\text{Sn-3Ag-0.5Cu-0.5Ce-0.5Ge}$  solder alloy air-stored at room temperature for 338 h increased gradually from 0.65 at.% at the start to 1.09 at.% at the end (Fig. 10). Furthermore, the amount of Ge on the  $\text{CeSn}_3$  intermetallic phase air-exposed at 150 °C for 15 min increased drastically to 1.23 at.%, and then increased again slightly to 1.31 at.% as storage time was extended to 146 h. The source of Ge enrichment may be the tendency of surface segregation for Ge atoms to diffuse outward from the interior of the  $\text{CeSn}_3$  phase and the Cu-Ge-Ce-Sn phase enveloping the  $\text{CeSn}_3$  clusters. Clearly, the addition of 0.5 wt.% Ge into  $\text{Sn-3Ag-0.5Cu-0.5Ce}$  alloy reduced the oxidation rate of the  $\text{CeSn}_3$  intermetallic phase in this solder. The rapid growth of whiskers in rare-earth-doped solder alloys has been attributed to oxidation of intermetallics containing rare earth elements, which provide the compressive stress needed to extrude tin atoms out of the oxide layer on intermetallic clusters [5,10–12]. It follows that reducing the oxidation reaction in  $\text{Sn-3Ag-0.5Cu-0.5Ce-0.5Ge}$  as a result of Ge-alloying leads to less driving force for whisker growth.

#### 4. Conclusions

Alloying solders with rare earth elements improve many performance aspects [21,22]. Unfortunately, rapid whisker growth for these alloys negates any beneficial effects [5,10–12]. This study presented a novel method for inhibiting tin-whisker growth by adding Ge into solder containing rare earth elements. Experimental results indicate that oxidation of  $\text{CeSn}_3$  intermetallic compounds in the  $\text{Sn-3Ag-0.5Cu-0.5Ce-0.5Ge}$  alloy can be largely reduced, leading to an insufficient number of tin atoms and insufficient compressive stress, both of which are needed for whisker growth on the surface of this solder alloy.

#### Acknowledgements

This work was sponsored by National Taiwan University, under Grant No. 96R0210, and by the National Science Council, Taiwan, under Grant No. NSC-96-2221-E002-150-MY3.

**References**

- [1] M.A. Dudek, R.S. Sidhu, N. Chawla, *JOM* 18 (2006) 57–62.
- [2] C.M.L. Wu, Y.W. Wong, *J. Mater. Sci.: Mater. Electron* 18 (2007) 77–91.
- [3] Y. Shi, J. Tian, H. Hao, Z. Xia, Y. Lei, F. Guo, *J. Alloys Compd.* 453 (2008) 180–184.
- [4] J.X. Wang, S.B. Xue, Z.J. Han, S.L. Yu, Y. Chen, Y.P. Shi, H. Wang, *J. Alloys Compd.* 467 (2009) 219–226.
- [5] T.H. Chuang, S.F. Yen, *J. Electron. Mater.* 35 (2006) 1621–1627.
- [6] W.C. Ellis, D.F. Gibbons, R.C. Treuting, in: R.H. Doremus, B.W. Roberts, D. Turnbull (Eds.), *Growth and Perfection of Crystal*, John Wiley & Sons, New York, 1958.
- [7] K.N. Tu, J.C.M. Li, *Mater. Sci. Eng. A* 409 (2005) 131–139.
- [8] K. Chen, G.D. Wilcox, *Phys. Rev. Lett.* 94 (2005) 066104.
- [9] S.H. Liu, C. Chen, P.C. Liu, T. Chou, *J. Appl. Phys.* 95 (2004) 7742–7747.
- [10] T.H. Chuang, *Scripta Mater.* 55 (2006) 983–986.
- [11] T.H. Chuang, S.F. Yen, *Mater. Forum* 539–543 (2007) 4019–4024.
- [12] T.H. Chuang, *Metall. Mater. Trans.* 38A (2007) 1048–1055.
- [13] M.A. Dudek, N. Chawla, *J. Electron. Mater.* 38 (2009) 210–220.
- [14] T.H. Chuang, H.J. Lin, *J. Electron. Mater.* 38 (2009) 420–424.
- [15] S.W. Cho, K. Han, Y.J. Yi, S.J. Kang, K.H. Yoo, K. Jeong, C.N. Whang, *Adv. Eng. Mater.* 8 (2006) 111–114.
- [16] R. Lee, W.S. Sin, J.K. Jeon, H.S. Kim, *IEEE Adv. Packag. Mater.: Processes Properties Interfaces* (2005) 121–125.
- [17] J.N. Lalena, N.F. Dean, M.W. Weiser, *Adv. Eng. Mater.* 31 (2002) 1244–1249.
- [18] G.L. Gong, A.P. Xian, *Acta Metall. SINICA* 43 (2007) 759–763.
- [19] K. Habu, N. Takeda, H. Watanabe, K. Ooki, J. Abe, T. Saito, Y. Taniguchi, K. Takayama, *IEEE Electron. Environ.* (1999) 21–24.
- [20] T.B. Massalski, J.L. Murray, L.H. Bennett, H. Baker, *Binary Alloy Phase Diagrams*, ASM, Metals Park, Ohio, 1986, pp. 705, 712, 742, 920, 1251.
- [21] M.A. Dudek, R.S. Sidhu, N. Chawla, M. Renavikar, *J. Electron. Mater.* 35 (2006) 2088–2097.
- [22] D.Q. Yu, J. Zhao, L. Wang, *J. Alloys Compd.* 376 (2004) 170–175.